Journal of
Marine Science and Engineering

MDPI

Article

Pulsatile Ventilation Flow in Polychaete *Alitta succinea* Burrows

Elizabeth A. K. Murphy and Matthew A. Reidenbach *

Department of Environmental Sciences, University of Virginia, Charlottesville, VA 22904, USA; eam6vf@virginia.edu
* Correspondence: mar5jj@virginia.edu

Abstract: In aquatic sediments, active ventilation of burrows is an important component of sediment metabolism, transporting solutes across the sediment–water interface. Within a burrow, the temporal and spatial structure of the flow velocity can dictate the flux of solutes across the burrow walls. However, it is difficult to measure the fine-scale flow dynamics within a burrow due to the opacity of marine sediments. Here, we allowed a nereid polychaete *Alitta succinea*, a cosmopolitan deposit feeder found in brackish to marine soft sediments, to construct burrows in a transparent, elastic sediment analog. This allowed the measurement of the temporal velocity structure of flow in the burrow using particle tracking velocimetry. We find that the flow within the burrow of this piston-pumping polychaete is unsteady and that oscillations in flow velocity are damped with distance along the tube. We also show that the flow velocity in a tube scales with worm size. Conversely, neither the unsteadiness of flow oscillations nor the stroke frequency of the worm pump scale with worm size.

Keywords: polychaete; bioirrigation; burrow ventilation; particle tracking velocimetry (PTV); fluid dynamics

Citation: Murphy, E.A.K.; Reidenbach, M.A. Pulsatile Ventilation Flow in Polychaete *Alitta succinea* Burrows. *J. Mar. Sci. Eng.* **2024**, *12*, 1037. https://doi.org/10.3390/jmse12071037

Academic Editor: Panagiotis D. Dimitriou

Received: 2 May 2024
Revised: 10 June 2024
Accepted: 15 June 2024
Published: 21 June 2024

1. Introduction

Because diffusion coefficients in water are orders of magnitude smaller than in air, many aquatic organisms, as well as internal physiological systems, rely on pumps to accomplish advective transport of solutes. Internal biological pumps transport solutes such as oxygen or nutrients throughout the body. Burrow- or tube-dwelling animals pump fluid through their tubes to transport solutes, and also particles such as plankton for filter feeding, a process referred to as burrow ventilation. Burrow-building organisms are important component of coastal ecosystems. The burrowing and burrow ventilation activities of these organisms alter the chemistry of sediments, transporting oxygen into otherwise anoxic sediments through diffusion across the burrow walls (in cohesive sediments) or advective transport (in permeable sediments) [1,2]. Much of the literature examining tube-dwelling water pumpers focuses on the energetics of filter feeding and the mechanics of particle capture [3–6]. However, burrow ventilation also occurs for respiratory purposes, and the transport of solutes across the sediment–water interface within the burrow is an important consequence of burrow ventilation regardless of purpose. Indeed, bioirrigation (the exchange of solutes between porewater and the water column due to burrow ventilation [7]) is thought to have been critical to stabilizing oxygen cycling and the planet's oxygen reservoir beginning in the early Cambrian [8]. Since burrowing organisms can enhance oxygen levels within their surrounding sediments, they are often considered ecosystem engineers [9]. In addition, the tube burrows themselves can alter benthic metabolism and oxygen fluxes, where tubes of polychaetes can act as an anchor to free-floating macroalgae, enhancing algal abundances on mudflats [10,11].

Mechanical forcing of fluid motion through tubes is a ubiquitous biological phenomenon, both externally, such as burrow-dwelling organisms, and internally, such as the circulatory system. Biological pumps occur in many different forms within organisms. Positive displacement pumps generate fluid motion with oscillating pistons, by contracting

the walls of a fluid-filled chamber, such as the valve-and-chamber pump of many vertebrate hearts, or by peristaltic waves moving along the tube walls. For the first two types, valves can ensure unidirectionality [12]. Peristalsis, such as the waves of contractions driving flow in intestines or in tunicates [13,14], essentially moves the chamber containing the volume of fluid along the tube. Biological pumps can also employ cilia or flagella to drive flow, such as bivalves and sponges, respectively [15,16]. Burrowers use appendages (e.g., shrimp pleopod beating [17]; polychaete parapodia beating [3]), cilia (e.g. polychaetes [18]; heart urchins [19]) or muscular body motions that are either undulatory (brittle stars [20]; polychaetes [21]) or peristaltic (polychaetes [22]) to pump water through their burrows. The biological pumps of burrow-dwelling filter feeders tend to operate at low pressures, with high pumping rates and low energy expenditure [23]. On the other hand, burrowers who ventilate for respiratory purposes operate at higher pressures, with much lower pumping volumes, than filter feeders [22]. Benthic macrofauna often prefer lower bulk density sediments when burrowing, with both burrowing and bioturbation behaviors observed to be faster and stronger in soft, low-bulk-density sediments, regardless of grain size [24].

For many species, pumping occurs intermittently, with periods of active burrow ventilation and periods of rest typically occurring on a scale of minutes to tens of minutes [3,25,26]. This intermittency has important consequences for the transport of solutes across the burrow walls [26]. Because undulatory burrow ventilation is characterized as a piston pump [4] (though this is called into question by Vogel (2007) [12], who suggests that the undulatory worm pump, as well as beating appendages, could also act as a peristaltic pump), it is likely that the flow in the burrow is unsteady. However, most studies of the flow dynamics of ventilating zoobenthos do not have high enough temporal resolution of flow data to measure unsteadiness of the flow [3,27], or, in the case of mud shrimp, find that the flow is steady [17].

On shorter temporal scales, unsteadiness of the flow during active pumping could be important for the energetics of the pump due to viscous interactions between the fluid and the burrow wall, especially at the burrow entrance. Oscillating shear stresses at the burrow wall may have implications for the microbial communities that inhabit sediments since pressure gradients within the burrow drive percolation into porous sediments, further influencing solute transport.

Though pressure characteristics, bulk volume flow rates and energetics of burrow ventilation have been reported for various species, because of the opacity of marine sediments, flow within worm tubes is difficult to quantify. Some studies have used artificial tubes, where pumping behavior and flow rate is observed through the walls of a glass or plastic tube, providing key insight into the mechanics of burrow ventilation [4]; however, this method has been shown in some cases to alter pumping behavior [21] and does not capture all of the physics within a worm tube, such as the elasticity of the walls of a tube constructed in natural sediment. Other studies have measured or modeled the flow rate at the burrow entrance or exit [25,28].

To address these limitations and to visualize flow within the tube during burrow ventilation, we use a transparent mud analog in which a common nereid polychaete, *Alitta succinea*, readily builds a burrow. Nereid polychaetes are common in coastal sediments, play an important role in nutrient cycling, and some species are an economically important bait fishery. *A. succinea* has been shown to set up oscillating redox conditions near the burrow wall due to ventilation activity [25]. Using simultaneous video recordings of particle movement in the burrow and pumping activity of the *A. succinea* individual, we are able to relate the pumping activity to the fluid mechanics in worms of a range of sizes. Specifically, this work addresses the following questions: (1) Is the flow in a piston-pumping polychaete burrow steady or unsteady?; (2) How do the pump characteristics and flow characteristics vary with worm size?

2. Materials and Methods

2.1. Polychaetes

Alitta succinea specimens and associated sediment were collected from the muddy intertidal zone on the Delmarva Peninsula of Virginia. USA. Polychaetes, in general, are found in high abundances but can be spatially and temporally variable [29] in these environments, with densities up to 7500 individuals m^{-2} [30]. *A. succinea* individuals were kept at room temperature (24 °C) in small plastic tubs filled with mud collected from the same location as the specimens overlain with aerated artificial saltwater (10 ppt) until use. Worms were not provided a dedicated food source during housing because, as detritovores [31,32], the mud provided for burrowing should give sufficient food for the short period (maximum 1 week) during which they were housed prior to experiments. This low salinity was chosen to match the salinity of the water used to create the mud analog (described below), which was kept low to optimize the refractive index matching between the agarose gelatin, water in the polychaete tube, and Nafion granules. The intertidal zone in which these animals are found on the Delmarva peninsula experiences a wide range of temperatures on seasonal and tidal time scales, with temperatures on mudflats in the same region ranging between 33.9 and −2.1 °C at 3 cm below the sediment surface over a year-long period [25]. *A. succinea* is found to inhabit a range of salinities and tolerate salinities down to 2.5 ppt [33], with ventilation behavior responding to salinities at the lower range of tolerance, but not the organism's oxygen consumption [34]. The specimens used here were collected from intertidal mudflats along the mainland side of Oyster Harbor. Salinity in Oyster Harbor has been measured every 1–3 months for 31 years and averages 29 ppt, ranging from 8.9 to 36 ppt [35]. Study animals ranged in size from 0.12 g to 1.05 g wet weight.

2.2. Mud Analog

We developed a transparent sandy mud analog in which our study species, *A. succinea*, readily built tubes. The goal was an optically transparent, nontoxic substrate that worms of a range of sizes would burrow into, and also be able and willing to build a semipermanent tube. Gelatin is often used in studies of the kinematics of burrowing by polychaetes [36,37]. However, for this study, a substrate with a closer refractive index match to water was desired. Therefore, low-density (0.04% by mass) agarose (Sigma-Aldrich, St. Louis, MO, USA), an elastic solid, was used, which has a refractive index of 1.333 [38]. Low-density agarose is also easily plastically deformed even at low stresses [39], so that the small specimens used in this study were able to build permanent burrows. However, smaller worms like the species used here have difficulty burrowing in a pure gelatin or agarose gel, likely due to being unable to generate enough friction to gain a purchase ([40] and personal observation). Therefore, to better mimic a sandy mud sediment, we added a relatively transparent granular substance to the agarose to simulate mud with a small amount of granular media. We used Nafion (C. G. Processing, Rockland, DE, USA), a nontoxic, optically transparent, hydrophilic fluoropolymer with a refractive index, when it has absorbed water, of 1.35 [41,42]. We used granular Nafion, 60–100 mesh (grain size 150–250 microns). Agarose gel was prepared by dissolving the agarose powder (4 g agarose per liter of 10 ppt saltwater) over heat. The dissolved agarose was then added to a narrow glass aquarium (20 × 20 × 5 cm), and granular Nafion was added to the solution. The solution was cooled to near room temperature while stirring, then placed in a freezer until set and then removed to room temperature until use within a few hours. The stirring of the agarose solution until setting helped the Nafion to not sink to the bottom of the aquarium before the gel set. Nafion was prepared by first boiling in deionized water until optically transparent, then salt water (10 ppt) and baking soda to neutralize it. This is necessary because Nafion is an ion exchange resin, and in contact with salt water, the cations exchange.

2.3. Experimental Setup

Once the agarose gel was set, artificial saltwater (10 ppt) was added and the aquarium was brought to room temperature (24 °C). An *A. succinea* individual was added to the aquarium, and allowed a maximum of 24 h to construct a burrow. The overlying water was aerated using an airstone during the burrow construction period. Worms were not provided a food source during ventilation experiments because it was important to maintain optical clarity within the experimental aquarium, and the time in the experimental aquarium was short. Particle tracking was used to measure flow velocity in the tube in front of and behind the worm. This system (Figure 1) consisted of a 300 mW green laser beam (532 nm wavelength) (Laserglow Technologies, Toronto, ON, Canada) passed through a convex lens (CVI Melles Griot Inc., Albuquerque, NM, USA), resulting in a thin sheet of laser light. Red fluorescent microsphere particles (peak wavelength 605 nm; fluoresce under 300–550 nm lasers), 63–75 microns in diameter, with a density of 0.985–1.005 g/cc (Cospheric LLC, Somis, CA, USA), were added to the water and video was recorded at 24 fps using a macro lens on a DSLR camera (Canon Rebel t2i; Canon Inc., Tokyo, Japan) with a 550 nm long wave pass edge filter (Andover Corp., Salem, NH, USA) affixed to the lens so that only the orange fluorescence from the particles could pass through. Simultaneously, video of the pumping activity of the worm was taken with either a DSLR camera (Nikon, Tokyo, Japan) or a video camera (Sony HDR-CX160, Sony Electronics Inc., San Diego, CA, USA), both at 24 fps. Video recordings were captured by the camera on an internal SD card and decomposed into a series of TIFF images of each frame using FFmpeg for analysis. An example frame and the tracked particles from that sequence are given in Figure 2. Because agarose is not perfectly transparent [38], flow data could only be taken when the burrow was constructed fairly close to the sides of the aquarium. A total of 5 individuals were used and a new aquarium with freshly made agarose was used for each individual.

Each individual was filmed over a maximum of 12 h. Most of this time was spent waiting for the animal to be in a good location for filming of the worm pump or visualization of particles; during the waiting periods between active filming, the overlying water was aerated with an airstone. During the brief intervals of active filming, aeration was ceased to minimize disturbance of the flow at the burrow entrance.

2.4. Analysis

Particles in the flow were tracked using the ImageJ particle tracking plugin MTrackJ [43]. Due to the no-slip condition at the walls of the burrow, the magnitude of the velocity varies across the diameter. Therefore, only particles near the middle of the burrow were tracked (Figure 2), to obtain the midline velocity in the burrow over time. The average flow in the burrow was estimated as half the midline velocity, which assumes a parabolic flow profile. When the flow in a tube is laminar (dominated by viscous forces as indicated by a low Reynolds number ($Re = \frac{vD}{\nu}$, where D is the tube diameter, v is the midline velocity, and ν is the kinematic viscosity)) and steady, the velocity is assumed to have a parabolic shape. This assumption may not entirely hold here due to the pulsatile nature of the flow [44]. Where visible, multiple particles were tracked at a given time and the average velocity at that time was taken. The velocity data over time was smoothed using a moving window of 0.2 s. Only sequences of longer than 2 s were analyzed for flow data. Flow recordings were taken both in front of the worm, between the head and the burrow entrance, with flow moving towards the worm, and behind the worm's tail, with flow moving away from the worm towards the burrow exit. Where possible, video was taken during pumping activity both in front of and behind the worm; however, the shape of the burrow or location of the worm precluded this in some cases. The worm pumping mechanics were determined by measuring the stroke frequency (Hz) of the pumping activity. Where video was able to be taken of the worm in the lateral orientation to the camera, the peak of the wave passing down the body was tracked through each pump stroke to measure the speed and length of the pump. Flow velocity measurements were taken for a total of 5 individuals, with

flow measurements made both behind and in front of the polychaete possible for 4 of the individuals. The worm pump characteristics were calculated for 4 of the individuals.

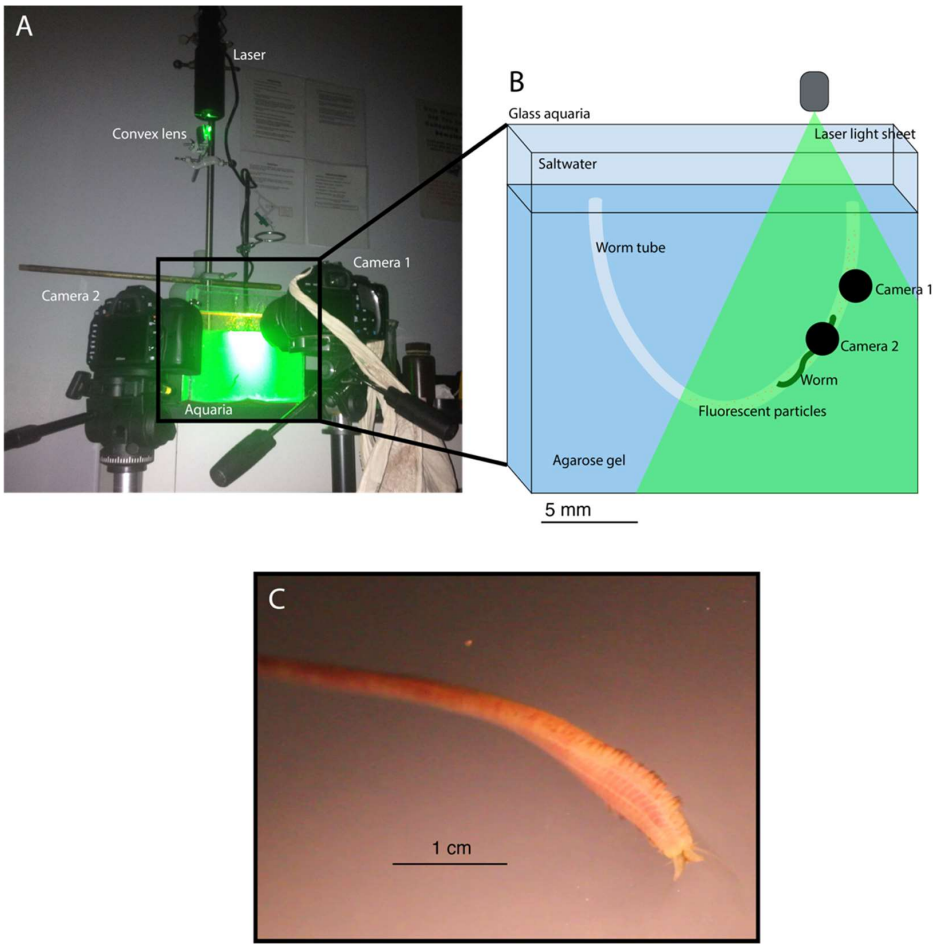

Figure 1. (**A**) Experimental setup. The camera on the right is recording particles in the burrow, and the camera on the left is recording the worm movements lower in the burrow. (**B**) A schematic of the experimental setup. The aquarium is 20 × 20 × 5 cm. (**C**) An image of an *A. succinea* individual burrowing in the agarose mixture. The individual is near the aquarium wall. This image was taken without the laser light sheet for better visibility.

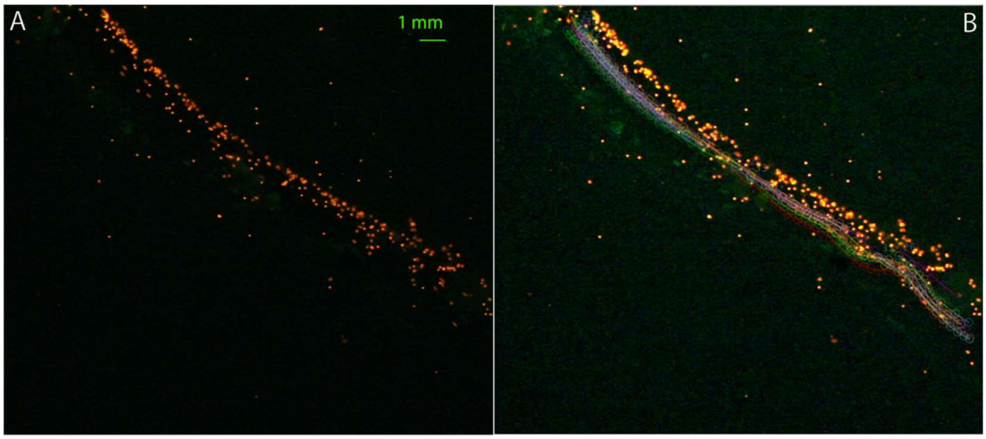

Figure 2. (**A**) A still frame from a video of particles being pumped through an *A. succinea* burrow. (**B**) The particle tracks (lines with circles) that were measured to calculate the midline velocity in the burrow over time.

3. Results

The individuals used in this study appeared to build burrows similar to what is observed in natural sediments in the laboratory and in situ, namely, U-shaped burrows built to a depth of between 10 and 20 cm, with a burrow diameter ranging from 1.7 to 3.6 mm [25,45–47]. We observed that the worms tended to pump with their head near (generally 2–5 cm from) a burrow opening and pump water down into that closest tube opening and out of the far opening. The kinematics of the worm pump varied with individuals, but the frequency of the undulatory wave that drives the flow stayed fairly consistent (Table 1). The number given in the individual columns in Tables 1 and 2 is unique to that individual.

Table 1. Kinematics of the worm pump. Table metrics include the following: individual (I), sequence, which matches a sequence number in Table 1, wet weight (W) of the specimen used, the average velocity of the undulatory wave driving flow (v_p) and the maximum v_p (calculated by finding the maximum speed of each wave tracked and taking the mean), the length traveled by the undulatory wave (L), and the pumping stroke frequency (f_p).

I	W (g)	Sequence	v_p (mm s^{-1})	v_p max (mm s^{-1})	L (mm)	f_p (Hz)
1	0.2	1	5.33	9.8	6.4	0.67
		4	11.16	16.35	-	0.77
2	0.12	5	7.05	8.83	5.17	0.77
3	0.17	6	8.64	11.58	6.97	0.77
4	1.05	8	13.68	18.78	20.8	0.77
5	0.38	-	-	-	-	-

Table 2. Worm pump and ventilation flow characteristics. Table metrics include the following: individual (I), wet weight (W), burrow diameter at the location of flow recording (D), time-averaged Reynolds number (Re), time-averaged volumetric flow rate (Q), time averaged midline velocity (v), velocity amplitude (v_a), measured as the peak–trough distance of the oscillations in v, the oscillation frequency (f_Q), and Womersley number (α). Note that the number given in the individual column corresponds to the numbered individuals in Table 1.

I	Sequence	Burrow Location	D (mm)	Re	Q (mm^3 s^{-1})	v (mm s^{-1})	v_a Amplitude (mm)	f_Q (Hz)	α
1	1	Near entrance	1.7	3.08	1.95	1.64	2.5	0.744	1.96
	3	Behind worm	1.9	13.60	9.29	6.65	3.5	0.93	2.37
2	4	Near entrance	3.1	6.73	7.60	2.00	3.4	0.78	3.57
	5	Behind worm	2.5	2.60	2.30	0.97	-	0	0
3	6	Near entrance	3.6	12.90	16.70	3.40	3.1	1.58	5.83
	7	Near entrance	2.3	8.70	7.10	3.60	4.4	0.744	2.53
4	8	Near entrance	2.5	15.80	14.20	5.90	5.0	0.488	2.26
	9	Behind worm	1.8	27.30	17.80	14.10	-	0	0
5	10	Behind worm	2.0	11.10	8.00	5.20	2.8	0.186	1.11
	11	Near entrance	2.0	12.30	8.80	5.70	3.6	1.02	2.60

The inflow of water to the worm pump is clearly pulsatile (Figure 3A). However, once past the worm pump, the flow becomes less pulsatile, with lower frequency and less-uniform oscillations (Figure 3B). In some of the recordings taken behind the polychaete, there was no discernible oscillations in the flow velocity (Table 2).

Figure 4A presents an example of flow velocity, taken along the midline of the tube from near the burrow entrance, showing the oscillatory nature of the unsteady flow. Figure 4B shows the wave speed of the worm pump from the anterior to posterior direction along the polychaete body, indicating the movement of the polychaete. As can be seen, the traveling waves of the undulating worm slow as they travel along the animal's body, roughly corresponding with the fall in velocity of the tube flow.

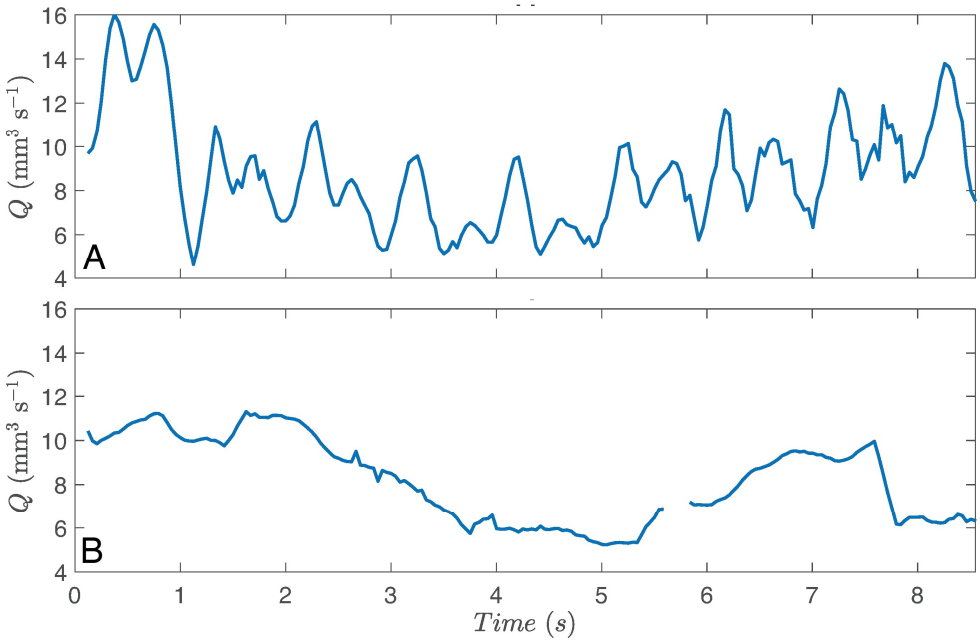

Figure 3. Volumetric flow rate in a burrow, near the entrance in front of the worm (**A**) and behind the worm tail (**B**). Data are from the same worm and burrow, but taken at different times. Worm was actively pumping during both sequences. Data from individual 5 (W = 0.38 g).

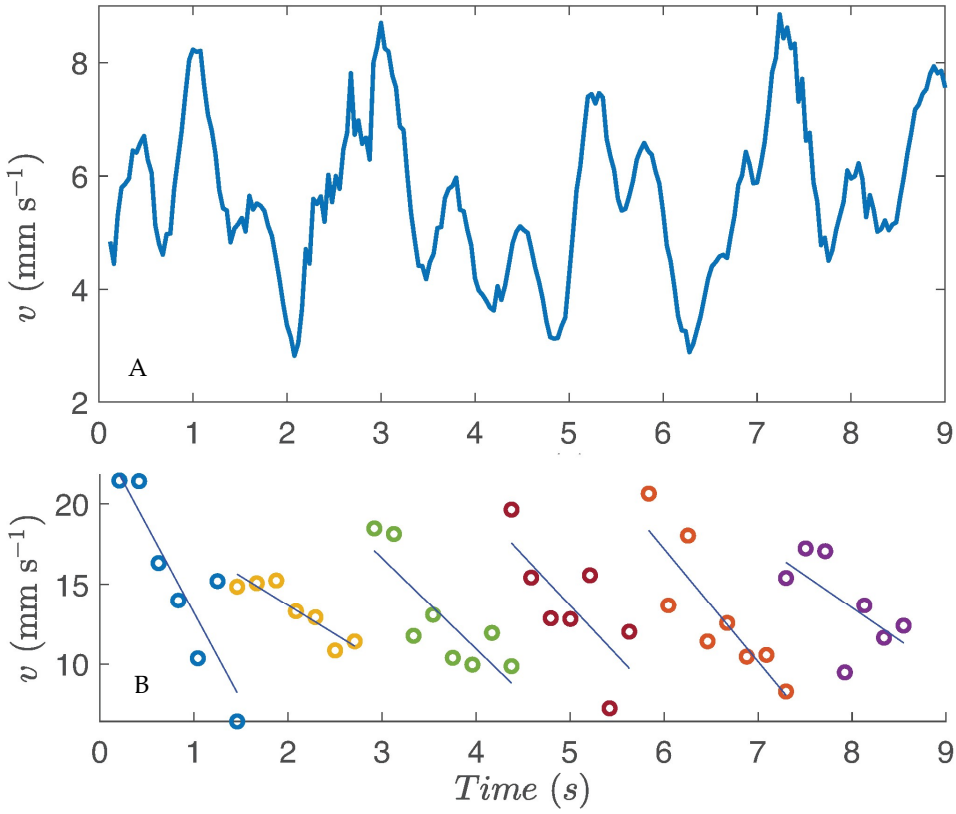

Figure 4. The midline flow velocity over time (**A**) in the section of a burrow near the entrance, in front of the worm, shown with the wave speed of the worm pump (**B**) which was recorded simultaneously with the flow velocity. Each color of open circle represents a single wave as it passed in the anterior to posterior direction along the polychaete body. The blue lines in (**B**) show a linear regression fit through the velocity data for each wave. Data from individual 4 (W = 1.05 g).

The time-averaged Reynolds number (*Re*) fluctuated over time within the laminar flow regime, in tandem with the velocity fluctuations (Figure 5). The time-averaged *Re* ranged over a factor of 10, between 2.6 and 27 (Table 2). Unsurprisingly, due to the linear dependence of *Re* on both the diameter of the tube and the velocity of the flow, the average *Re* of the system increased with increasing worm size (Table 2). The average flow velocity (v) and volumetric flow rate (Q) also increase with worm size (Figure 6).

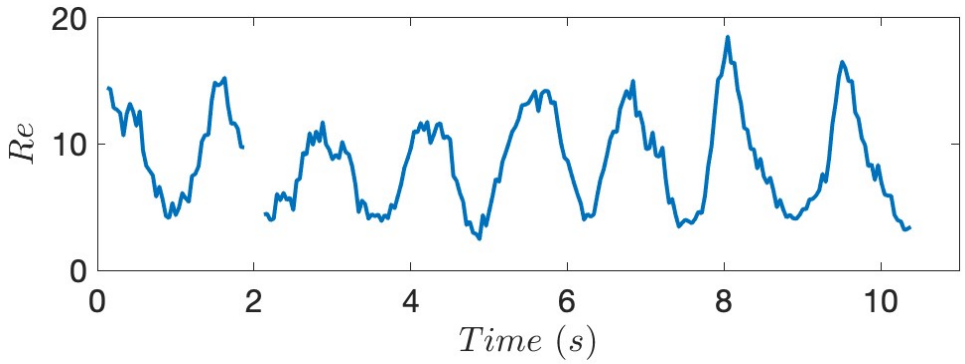

Figure 5. An example of Reynolds number (Re) fluctuating over time near the entrance to the worm tube. Data from individual 3 (W = 0.17 g).

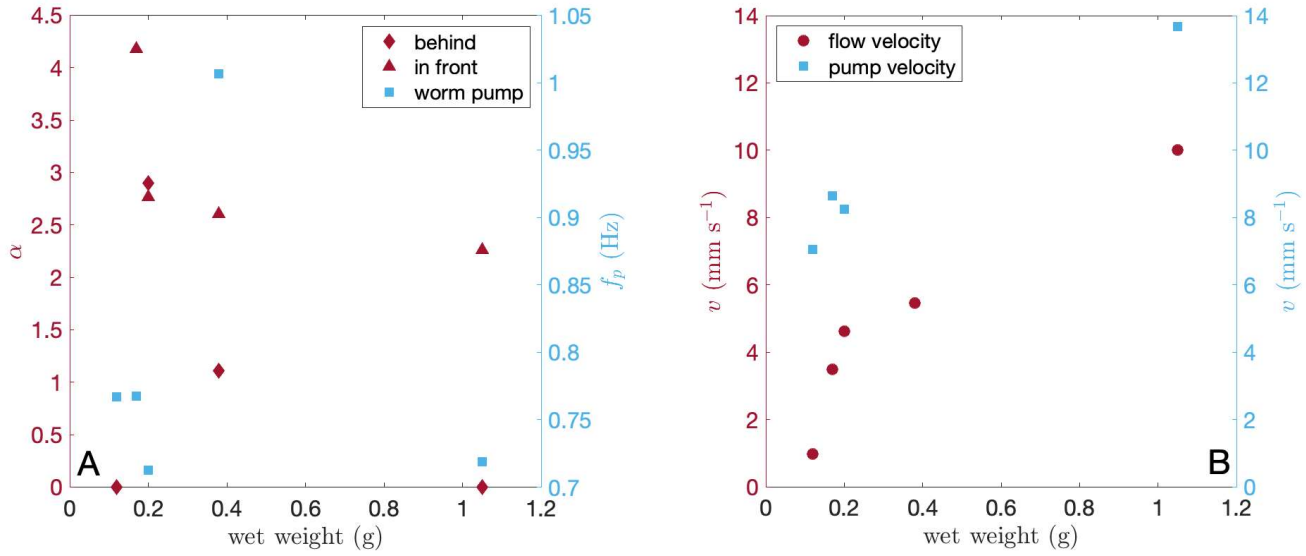

Figure 6. The Womersley number (α) of the flow (red) and the frequency of the worm pump (f_p) (blue) plotted against the wet weight of the polychaete (**A**). For α, it is separated by location in the burrow at which it was measured (behind the worm and in front of the worm). The variability of the midline flow velocity (v) (red) and the velocity of the pumping wave (v) (blue) with the worm weight are shown in (**B**). Pseudoreplicates (multiple measurements for one individual polychaete) were averaged.

The Womersley number (α) is a measure of the ratio of unsteady inertial forces to viscous forces in pulsatile tubular flow [48], similarly to the Reynolds number, and is useful for comparing pumps across sizes and in different systems and can predict the shape of the velocity profile of pulsatile flow across the diameter of a tube. The Womersley number is calculated as follows:

$$\alpha = r\sqrt{\frac{\omega}{\nu}} \quad (1)$$

where r is the tube radius, ω is the angular frequency of the unsteady flow (where $\omega = 2\pi f_Q$ and f_Q is the frequency of the volumetric flow unsteadiness in Hz), and ν is the kinematic

viscosity. The Womersley number is derived from the equation of motion for pulsatile flow driven by an oscillating pressure gradient. We calculated f_Q by taking a fast Fourier transform (FFT) of the time series. A larger value of α indicates that the flow in a tube is dominated by unsteady inertial forces, a thinner boundary layer at the tube walls, and a less parabolic shape to the velocity profile across the tube, whereas a lower value indicates viscous dominance and a parabolic velocity profile, and therefore a thicker boundary layer along the walls of the tube. The flow is considered quasi-steady at $\alpha < 1$ [44]. The Womersley number behind the worm pump ranges from 0 (no discernible pulsatile flow) to 2.37 and the Womersley number in front of the worm pump ranges from 1.96 to 5.83, indicating that the flow in the worm tube can either be in a quasi-steady state or the intermediate region [49]. Both regions of the tube exhibit a range of flow frequencies, with the region behind the worm appearing to have a lower frequency, even in some instances having no discernible velocity oscillations (Figure 6A). The frequency of the pumping waves also do not appear to vary with worm size. However, the velocity of the flow as well as the velocity of the pumping wave do both appear to increase with worm size (Figure 6B).

4. Discussion

The variation in the Womersley number does not seem to be driven by the size of the worms (Figure 6). In quasi-steady state, where $\omega < 1$, which we only observed occuring in some cases behind the worm, never at the inflow, there is dominance of viscous forces and the pressure oscillations and velocity oscillations are phase matched rather than lagged [50]. The low Womersley numbers here also indicate that the flow should be parabolic, with steep velocity gradients at the wall, rather than the plug flow, which would occur with increased Womersley number [50]. The unsteadiness of the flow entering the burrow could have implications for mass transport across the walls of the burrow [25]. Higher Womersley number flows have been shown to result in steeper velocity gradients at the burrow wall, increasing heat and mass transfer. In addition, pulsatile flows can impact the chemoreception of organisms, and result in discreet odor samples, a strategy used by organisms that "sniff" [50]. Some burrow-dwellers are known to gather chemical information through burrow ventilation [51], and flow unsteadiness is thought to be important to the transport of chemical cues [52]. In addition, we observed the burrow walls at the location of the worm pump expanding and contracting as the pressure in the tube pulsed with the pumping. Because marine muds are also elastic solids, it is likely that this occurs in situ as well, and is another reason that using rigid artificial tubes to estimate flow parameters could give erroneous results.

Previous work on polychaete burrow ventilation has measured flow rates and pressure characteristics for peristaltic pumpers *Arenicola marina* [22], other nereid species [27], and *Chaetopterus* [5], all of which are also described as a piston pump, using peristalsis of the body wall, undulatory body waves, or beating parapodia, respectively, to drive the flow in its tube. The worms used in the present study were much smaller than the specimens used in studies of other nereid worm pumps [3], and there are few flow measurements of flow for zoobenthos of this size [5,53]. For juvenile bivalves, with a lower velocity range and *Re* than the worm tubes measured here, the increased resistance to flow of the small diameter of the siphon tube results in greater relative energy expenditure for juvenile clams than adults [53]. In the case of the nereid polychaetes investigated in this study, the relative increase in resistance due to small tube diameter may be more acute due to the unsteadiness of the flow and the length of the worm tube. While we do not have precise measures of the length of tubes built by the individuals in our study, we observed ventilated tubes built to at least 10 cm depth in the aquarium. Viscous interactions with the tube wall increase when the flow is unsteady, resulting in an increase in energy expenditure to power this unsteady flow. The total power expenditure due to pumping is the sum of the unsteady power expenditure plus the baseline power expenditure of steady flow within the tube [17].

For unsteady flows in the relatively long tubes of *A. succinea*, the additional power expenditure to the flow unsteadiness may be significant. The bigger the amplitude of the

imposed velocity oscillation, as well as the bigger the tube diameter, the greater is the loss of energy to unsteadiness. Species of burrowing shrimp seem to actively maintain steady flow in the burrow, despite acting as a piston-like pump, possibly to save energy loss due to unsteady flow [17]. The individuals used in the present study, while covering a range of sizes (based on wet weight), do not encompass the entire size range of the species, instead skewing larger than natural populations. Two previous studies [25,54] surveyed *A. succinea* from mudflats in the same region as the present study. Individuals collected during these two studies ranged in size from 0.0254 to 0.4429 g and 0.025 to 0.35 g, respectively. The larger size range used here allowed for easier visualization of flow within burrows, but further work could investigate the pumping kinematics and flow dynamics of smaller individuals, which may be more constrained by viscous dissipation of energy along the walls of the tube.

It must be noted that *A. succinea* is a detritovore, ventilating its burrow solely for metabolic reasons and not for filter feeding. Filter feeders must pump a much greater volume of water through the tube, and, thus, may have different flow characteristics within the burrow [55]. Further, the leaky pump characteristic of *A. succinea* may not be the same as other nereid polychaetes, where backflow in the pump might be limited by additional body waves and therefore the unsteadiness of the flow may be reduced or eliminated [56]. Therefore, the results presented here are not necessarily applicable across a wide range of species.

5. Conclusions

We present a novel method of imaging unsteady flow in polychaete worm burrows. We show that in small nereid polychaete burrows, flow, especially at the burrow entrance, is pulsatile. This species does not build a tube that protrudes above the sediment–water interface; therefore, the burrow entrance acts as a drain flow. Pulsatile flow at the burrow entrance has implications for the energy losses to pipe entry, and, therefore, the metabolic cost of ventilation [28]. Pulsatile flow also alters the dispersion of solutes and particles through the pipe, as well as the diffusion of solutes across the burrow wall. Previous work has found that polychaete burrows, and the active pumping by the animals, alter the rates of oxygen flux across the burrow wall [25], which can likely impact bulk oxygen exchange with the overlying water column [57]. Future work should examine the impact of polychaete densities on solute fluxes (particularly oxygen) in muddy coastal sediments and across a wider range of worm sizes in order to estimate the size dependence of pump characteristics and mass transport for this species.

Author Contributions: Conceptualization, E.A.K.M. and M.A.R.; formal analysis, E.A.K.M. and M.A.R.; funding acquisition, M.A.R.; investigation, E.A.K.M.; methodology, E.A.K.M. and M.A.R.; supervision, M.A.R.; writing—original draft, E.A.K.M.; writing—review and editing, E.A.K.M. and M.A.R. All authors have read and agreed to the published version of the manuscript.

Funding: This research was funded by the National Science Foundation (NSF) through grants for the Virginia Coast Reserve Long-Term Ecological Research program (DEB-1237733 and DEB-1832221).

Institutional Review Board Statement: Not applicable.

Data Availability Statement: The data presented in this study are openly available via the Environmental Data Initiative data portal at https://doi.org/10.6073/pasta/4e3425fe68a4f0be4b257cdb973e9fbe; reference number VCR24402 (accessed on 2 May 2024).

Conflicts of Interest: The authors declare no conflicts of interest.

References

1. Welsh, D.T. It's a Dirty Job but Someone Has to Do It: The Role of Marine Benthic Macrofauna in Organic Matter Turnover and Nutrient Recycling to the Water Column. *Chem. Ecol.* **2003**, *19*, 321–342. [CrossRef]
2. Kristensen, E. Organic Matter Diagenesis at the Oxic/Anoxic Interface in Coastal Marine Sediments, with Emphasis on the Role of Burrowing Animals. *Hydrobiologia* **2000**, *426*, 1–24. [CrossRef]

3. Riisgård, H.U.; Vedel, A.; Boye, H.; Larsen, P.S. Filter-Net Structure and Pumping Activity in the Polychaete Nereis Diversicolor: Effects of Temperature and Pump-Modelling. *Mar. Ecol. Prog. Ser.* **1992**, *83*, 79–89. [CrossRef]
4. Riisgaard, H.U.; Larsen, P.S. Filter-Feeding in Marine Macro-Invertebrates: Pump Characteristics, Modelling and Energy Cost. *Biol. Rev.* **1995**, *70*, 67–106. [CrossRef] [PubMed]
5. Riisgård, H. Properties and Energy Cost of the Muscular Piston Pump in the Suspension Feeding Polychaete *Chaetopterus variopedatus*. *Mar. Ecol. Prog. Ser.* **1989**, *56*, 157–168. [CrossRef]
6. Jørgensen, C.B.; Famme, P.; Kristensen, H.S.; Larsen, P.S.; Møhlenberg, F.; Riisgård, H. The Bivalve Pump. *Mar. Ecol. Prog. Ser.* **1986**, *34*, 69–77. [CrossRef]
7. Kristensen, E.; Penha-Lopes, G.; Delefosse, M.; Valdemarsen, T.; Quintana, C.O.; Banta, G.T. What Is Bioturbation? The Need for a Precise Definition for Fauna in Aquatic Sciences. *Mar. Ecol. Prog. Ser.* **2012**, *446*, 285–302. [CrossRef]
8. Boyle, R.; Dahl, T.W.; Dale, A.W.; Shields-Zhou, G.; Zhu, M.; Brasier, M.; Canfield, D.E.; Lenton, T.M. Stabilization of the Coupled Oxygen and Phosphorus Cycles by the Evolution of Bioturbation. *Nat. Geosci.* **2014**, *7*, 671–676. [CrossRef]
9. Byers, J.E.; Grabowski, J.H. Soft-Sediment Communities. In *Marine Community Ecology and Conservation*; Sinauer Associates, Inc.: Sunderland, MA, USA, 2014; pp. 227–249.
10. Besterman, A.F.; McGlathery, K.J.; Reidenbach, M.A.; Wiberg, P.L.; Pace, M.L. Predicting Benthic Macroalgal Abundance in Shallow Coastal Lagoons from Geomorphology and Hydrologic Flow Patterns. *Limnol. Oceanogr.* **2021**, *66*, 123–140. [CrossRef]
11. Volaric, M.; Berg, P.; Reidenbach, M. An Invasive Macroalga Alters Ecosystem Metabolism and Hydrodynamics on a Tidal Flat. *Mar. Ecol. Prog. Ser.* **2019**, *628*, 1–16. [CrossRef]
12. Vogel, S. Living in a Physical World X. Pumping Fluids through Conduits. *J. Biosci.* **2007**, *32*, 207–222. [CrossRef]
13. Hennig, G.; Costa, M.; Chen, B.; Brookes, S. Quantitative Analysis of Peristalsis in the Guinea-Pig Small Intestine Using Spatio-Temporal Maps. *J. Physiol.* **1999**, *517*, 575–590. [CrossRef] [PubMed]
14. Waldrop, L.; Miller, L. Large-Amplitude, Short-Wave Peristalsis and Its Implications for Transport. *Biomech. Model. Mechanobiol.* **2016**, *15*, 629–642. [CrossRef]
15. Larsen, P.S.; Riisgåd, H.U. The Sponge Pump. *J. Theor. Biol.* **1994**, *168*, 53–63. [CrossRef]
16. Jørgensen, C.B.; Larsen, P.S.; Møhlenberg, F.; Riisgård, H.U. The Mussel Pump: Properties and Modelling. *Mar. Ecol. Prog. Ser.* **1988**, *45*, 205–216. [CrossRef]
17. Stamhuis, E.J.; Videler, J.J. Burrow Ventilation in the Tube-Dwelling Shrimp *Callianassa subterranea* (Decapoda: Thalassinidea): II. The Flow in the Vicinity of the Shrimp and the Energetic Advantages of a Laminar Non-Pulsating Ventilation Current. *J. Exp. Biol.* **1998**, *201*, 2159–2170. [CrossRef]
18. Quintana, C.O.; Hansen, T.; Delefosse, M.; Banta, G.; Kristensen, E. Burrow Ventilation and Associated Porewater Irrigation by the Polychaete *Marenzelleria viridis*. *J. Exp. Mar. Biol. Ecol.* **2011**, *397*, 179–187. [CrossRef]
19. Hollertz, K. Feeding Biology and Carbon Budget of the Sediment-Burrowing Heart Urchin *Brissopsis lyrifera* (Echinoidea: Spatangoida). *Mar. Biol.* **2002**, *140*, 959–969. [CrossRef]
20. Vopel, K.; Thistle, D.; Rosenberg, R. Effect of the Brittle Star *Amphiura filiformis* (Amphiuridae, Echinodermata) on Oxygen Flux into the Sediment. *Limnol. Oceanogr.* **2003**, *48*, 2034–2045. [CrossRef]
21. Kristensen, E. Oxygen and Carbon Dioxide Exchange in the Polychaete *Nereis virens*: Influence of Ventilation Activity and Starvation. *Mar. Biol.* **1989**, *101*, 381–388. [CrossRef]
22. Riisgård, H.; Berntsen, I.; Tarp, B. The Lugworm (*Arenicola marina*) Pump: Characteristics, Modelling and Energy Cost. *Mar. Ecol. Prog. Ser.* **1996**, *138*, 149–156. [CrossRef]
23. Riisgård, H.; Ivarsson, N. The Crown-Filament Pump of the Suspension-Feeding Polychaete *Sabella penicillus*: Filtration, Effects of Temperature, and Energy Cost. *Mar. Ecol. Prog. Ser.* **1990**, *62*, 249–257. [CrossRef]
24. Wiesebron, L.E.; Steiner, N.; Morys, C.; Ysebaert, T.; Bouma, T.J. Sediment Bulk Density Effects on Benthic Macrofauna Burrowing and Bioturbation Behavior. *Front. Mar. Sci.* **2021**, *8*, 707785. [CrossRef]
25. Murphy, E.A.K.; Reidenbach, M.A. Oxygen Transport in Periodically Ventilated Polychaete Burrows. *Mar. Biol.* **2016**, *163*, 208. [CrossRef]
26. Volkenborn, N.; Meile, C.; Polerecky, L.; Pilditch, C.; Norkko, A.; Norkko, J.; Hewitt, J.; Thrush, S.; Wethey, D.; Woodin, S. Intermittent Bioirrigation and Oxygen Dynamics in Permeable Sediments: An Experimental and Modeling Study of Three Tellinid Bivalves. *J. Mar. Res.* **2012**, *70*, 794–823. [CrossRef]
27. Kristensen, E. Ventilation and Oxygen Uptake by Three Species of *Nereis* (Annelida: Polychaeta). I. Effects of Hypoxia. *Mar. Ecol. Prog. Ser.* **1983**, *12*, 289–297. [CrossRef]
28. Jumars, P.A. Boundary-Trapped, Inhalant Siphon and Drain Flows: Pipe Entry Revisited Numerically. *Limnol. Oceanogr. Fluids Environ.* **2013**, *3*, 21–39. [CrossRef]
29. Hogan, S.; Reidenbach, M.A. Quantifying Tradeoffs in Ecosystem Services Under Various Oyster Reef Restoration Designs. *Estuaries Coasts* **2022**, *45*, 677–690. [CrossRef]
30. Hogan, S. Influence of Oyster Reefs on Infauna and Sediment Spatial Distributions within Intertidal Mudflats. *Mar. Ecol. Prog. Ser.* **2022**, *686*, 91–106. [CrossRef]
31. Jumars, P.A.; Dorgan, K.M.; Lindsay, S.M. Diet of Worms Emended: An Update of Polychaete Feeding Guilds. *Annu. Rev. Mar. Sci.* **2015**, *7*, 497–520. [CrossRef] [PubMed]

32. Neuhoff, H.-G. Influence of Temperature and Salinity on Food Conversion and Growth of Different *Nereis* Species (Polychaeta, Annelida). *Mar. Ecol. Prog. Ser.* **1979**, *1*, 255–262. [CrossRef]
33. Freel, R.W.; Medler, S.G.; Clark, M.E. Solute Adjustments in the Coelomic Fluid and Muscle Fibers of a Euryhaline Polychaete, *Neanthes Succinea*, Adapted to Various Salinities. *Biol. Bull.* **1973**, *144*, 289–303. [CrossRef]
34. Kristensen, E. Ventilation and Oxygen Uptake by Three Species of Nereis (Annelida: Polychaeta). II. Effects of Temperature and Salinity Changes. *Mar. Ecol. Prog. Ser.* **1983**, *12*, 299–306. [CrossRef]
35. McGlathery, K.J.; Christian, R.R. Water Quality Sampling—Integrated Measurements for the Virginia Coast, 1992–2023. Available online: https://portal.edirepository.org/nis/mapbrowse?packageid=knb-lter-vcr.247.18 (accessed on 30 April 2024).
36. Dorgan, K.M.; Jumars, P.A.; Johnson, B.; Boudreau, B.P.; Landis, E. Burrow Extension by Crack Propagation. *Nature* **2005**, *433*, 475. [CrossRef] [PubMed]
37. Murphy, E.A.K.; Dorgan, K.M. Burrow Extension with a Proboscis: Mechanics of Burrowing by the Glycerid *Hemipodus simplex*. *J. Exp. Biol.* **2011**, *214*, 1017–1027. [CrossRef] [PubMed]
38. Byron, M.L.; Variano, E.A. Refractive-Index-Matched Hydrogel Materials for Measuring Flow-Structure Interactions. *Exp. Fluids* **2013**, *54*, 1456. [CrossRef]
39. Normand, V.; Lootens, D.; Amici, E.; Plucknett, K.; Aymard, P. New Insight into Agarose Gel Mechanical Properties. *Biomacromolecules* **2000**, *1*, 730–738. [CrossRef] [PubMed]
40. Dorgan, K.M. Kinematics of Burrowing by Peristalsis in Granular Sands. *J. Exp. Biol.* **2018**, *221*, jeb167759. [CrossRef] [PubMed]
41. Downie, H.; Holden, N.; Otten, W.; Spiers, A.J.; Valentine, T.A.; Dupuy, L.X. Transparent Soil for Imaging the Rhizosphere. *PLoS ONE* **2012**, *7*, e44276. [CrossRef] [PubMed]
42. Leis, A.P.; Schlicher, S.; Franke, H.; Strathmann, M. Optically Transparent Porous Medium for Nondestructive Studies of Microbial Biofilm Architecture and Transport Dynamics. *Appl. Environ. Microbiol.* **2005**, *71*, 4801–4808. [CrossRef] [PubMed]
43. Meijering, E.; Dzyubachyk, O.; Smal, I. Chapter Nine—Methods for Cell and Particle Tracking. In *Methods in Enzymology*; Conn, P.M., Ed.; Imaging and Spectroscopic Analysis of Living Cells; Academic Press: Cambridge, MA, USA, 2012; Volume 504, pp. 183–200.
44. Vogel, S. *Life in Moving Fluids: The Physical Biology of Flow—Revised and Expanded*, 2nd ed.; Princeton University Press: Princeton, NJ, USA, 2020; ISBN 978-0-691-21297-5.
45. Bartoli, M.; Nizzoli, D.; Welsh, D.T.; Viaroli, P. Short-Term Influence of Recolonisation by the Polycheate Worm *Nereis Succinea* on Oxygen and Nitrogen Fluxes and Denitrification: A Microcosm Simulation. *Hydrobiologia* **2000**, *431*, 165–174. [CrossRef]
46. Swan, B.; Watts, J.; Reifel, K.; Hurlbert, S. Role of the Polychaete *Neanthes succinea* in Phosphorus Regeneration from Sediments in the Salton Sea, California. *Hydrobiologia* **2007**, *576*, 111–125. [CrossRef]
47. Kristensen, E. Direct Measurement of Ventilation and Oxygen Uptake in Three Species of Tubicolous Polychaetes (*Nereis* Spp.). *J. Comp. Physiol. B* **1981**, *145*, 45–50. [CrossRef]
48. Womersley, J.R. Method for the Calculation of Velocity, Rate of Flow and Viscous Drag in Arteries When the Pressure Gradient Is Known. *J. Physiol.* **1955**, *127*, 553–563. [CrossRef] [PubMed]
49. Özdinç Çarpinlioğlu, M.; Yaşar Gündoğdu, M. A Critical Review on Pulsatile Pipe Flow Studies Directing towards Future Research Topics. *Flow Meas. Instrum.* **2001**, *12*, 163–174. [CrossRef]
50. Loudon, C.; Tordesillas, A. The Use of the Dimensionless Womersley Number to Characterize the Unsteady Nature of Internal Flow. *J. Theor. Biol.* **1998**, *191*, 63–78. [CrossRef] [PubMed]
51. Smee, D.L.; Weissburg, M.J. Hard Clams (*Mercenaria mercenaria*) Evaluate Predation Risk Using Chemical Signals from Predators and Injured Conspecifics. *J. Chem. Ecol.* **2006**, *32*, 605–619. [CrossRef] [PubMed]
52. Webster, D.R.; Weissburg, M.J. The Hydrodynamics of Chemical Cues Among Aquatic Organisms. *Annu. Rev. Fluid Mech.* **2009**, *41*, 73–90. [CrossRef]
53. Du Clos, K.T.; Jiang, H. Overcoming Hydrodynamic Challenges in Suspension Feeding by Juvenile *Mya arenaria* Clams. *J. R. Soc. Interface* **2018**, *15*, 20170755. [CrossRef] [PubMed]
54. Kersey Sturdivant, S.; Perchik, M.; Brill, R.W.; Bushnell, P.G. Metabolic Responses of the Nereid Polychaete, *Alitta Succinea*, to Hypoxia at Two Different Temperatures. *J. Exp. Mar. Biol. Ecol.* **2015**, *473*, 161–168. [CrossRef]
55. Riisgard, H.U. Suspension Feeding in the Polychaete *Nereis diversicolor*. *Mar. Ecol. Prog. Ser* **1991**, *70*, 19–37. [CrossRef]
56. Riisgård, H.U.; Larsen, P. Water Pumping and Analysis of Flow in Burrowing Zoobenthos: An Overview. *Aquat. Ecol.* **2005**, *39*, 237–258. [CrossRef]
57. Volaric, M.P.; Berg, P.; Reidenbach, M.A. Oxygen Metabolism of Intertidal Oyster Reefs Measured by Aquatic Eddy Covariance. *Mar. Ecol. Prog. Ser.* **2018**, *599*, 75–91. [CrossRef]